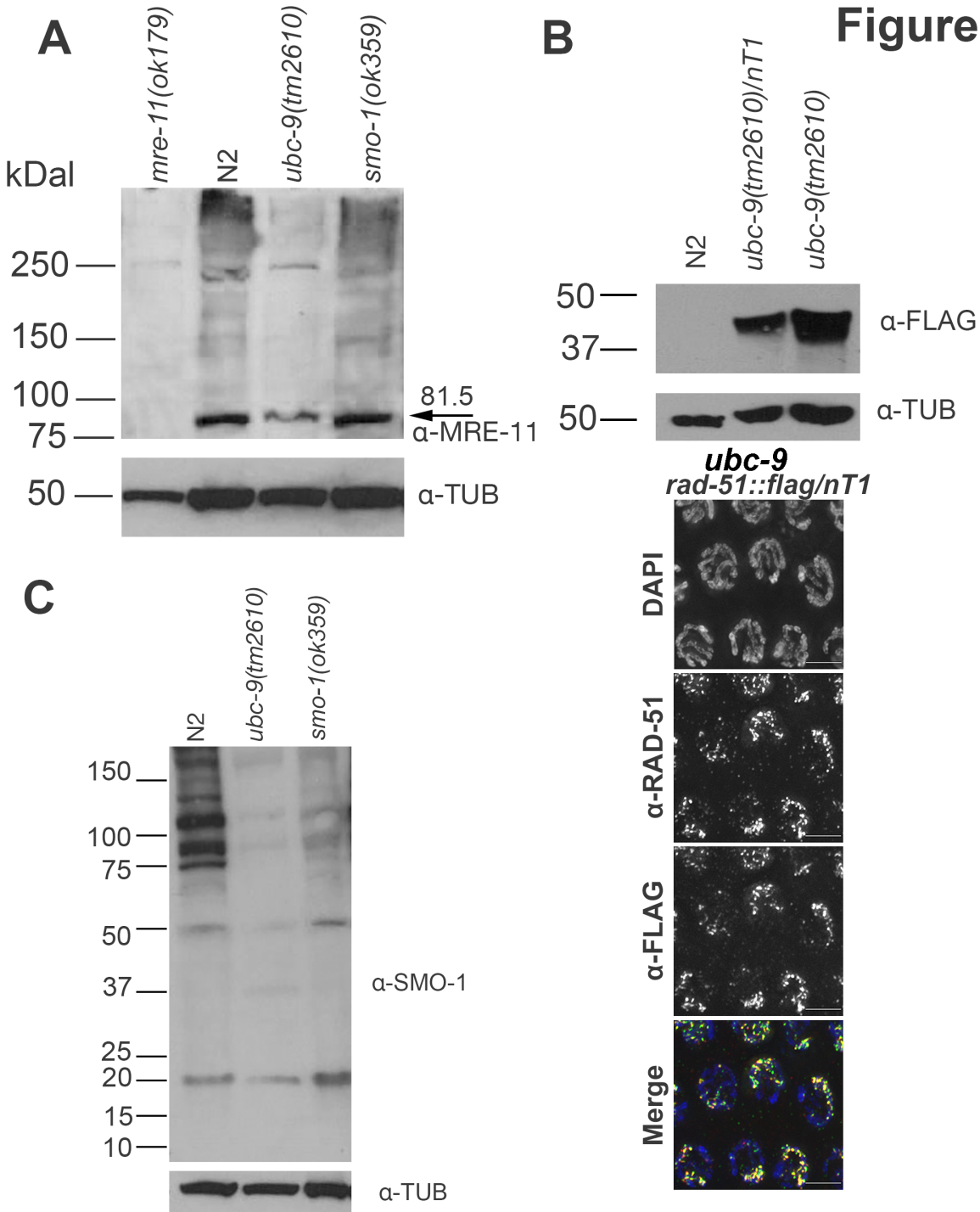


Mitotic and meiotic functions for the SUMOylation pathway in the *Caenorhabditis elegans* germline

Reichman Rachel*, Shi Zhuoyue*, Malone Robert* and Smolikove Sarit*[†]

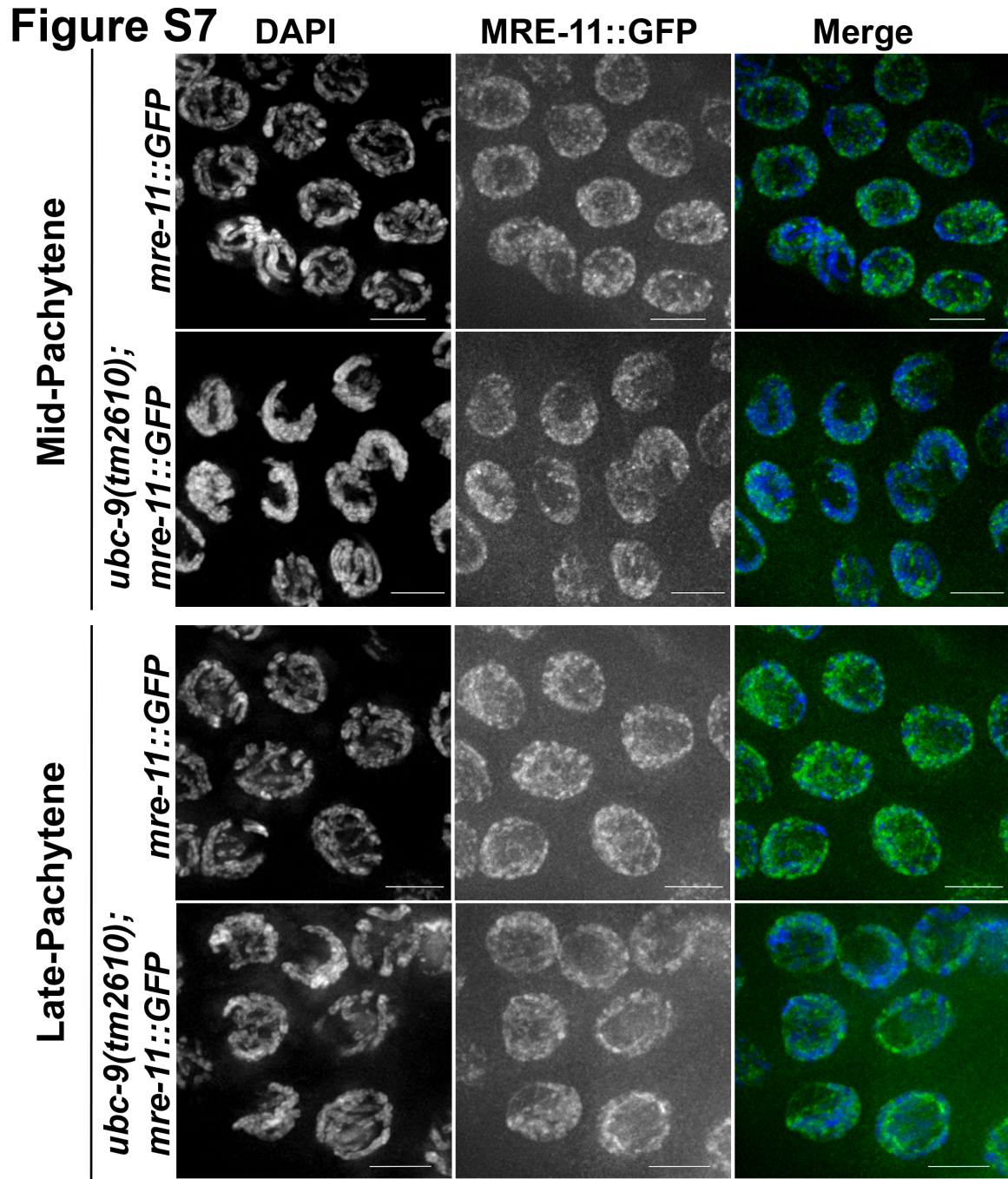
Supplementary figures 6-10

Figure S6



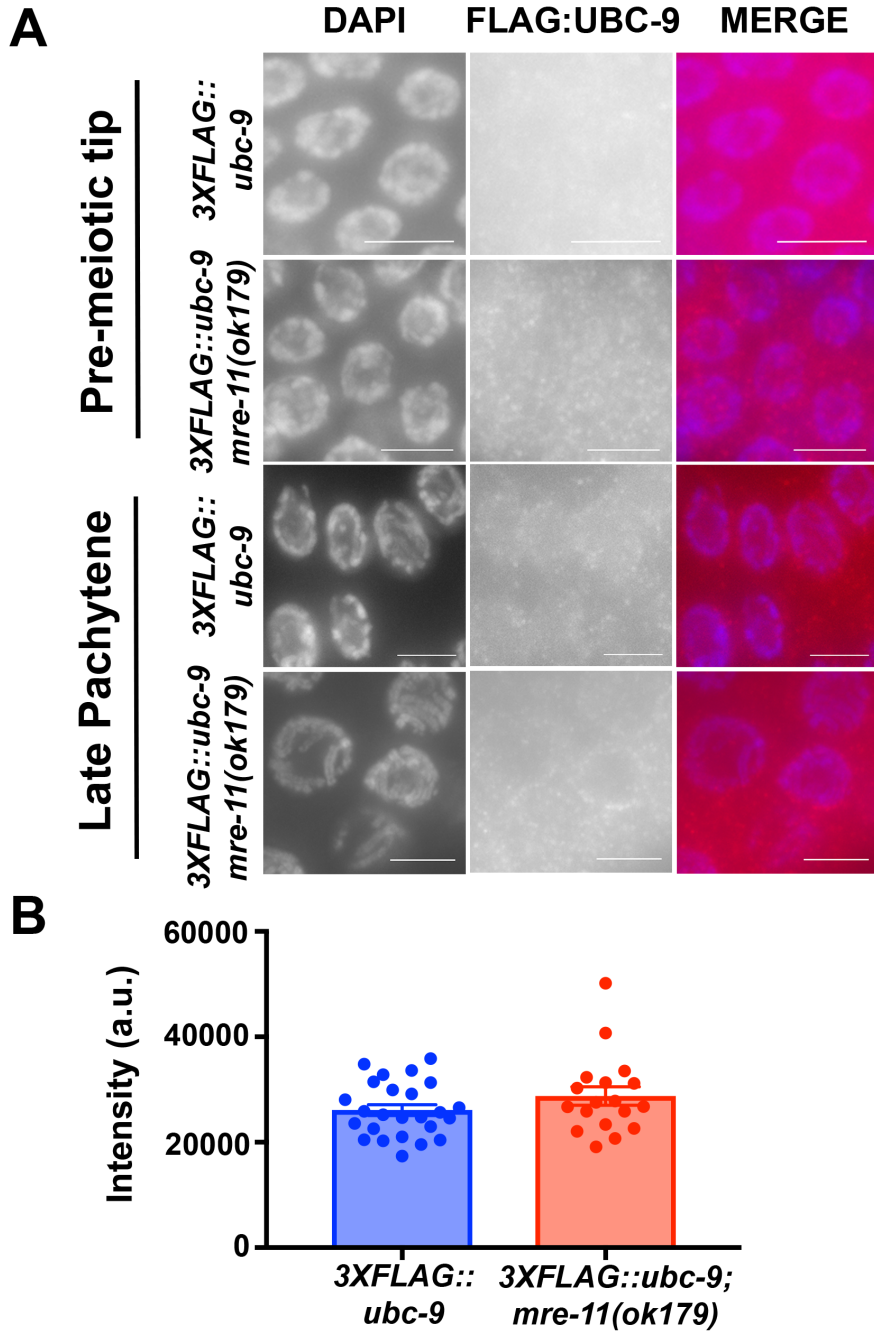
Supplemental Figure 6: MRE-11 and RAD-51 protein levels and molecular weight are unchanged in SUMOylation mutants, but SMO-1 is reduced. A) Western blot for endogenous MRE-11 (arrow points to MRE-11 band). There is no noticeable difference in the

position of the MRE-11 band in wild type or either SUMO mutant. Worm lysates were prepared with N-Ethylmaleimide (NEM) that blocks deSUMOylation of proteins. B) Western blot of total RAD-51::3XFLAG protein probed with a α -FLAG antibody. RAD-51::3XFLAG levels are similar in *ubc-9(tm2610)* and balanced strains, even though there are increased RAD-51 foci observed in the germline. RAD-51::3XFLAG is on the non-balancer chromosome IV, resulting in balanced worms having less RAD-51::3XFLAG than homozygous worms. C) Lines containing *rad-51::flag* were co-stained with both α -RAD-51 and α -FLAG. Complete overlap of the two stains indicates that RAD-51::FLAG localizes normally to sites of DNA damage. Images are of early to mid pachytene in both balanced and homozygous *rad-51::flag; ubc-9(tm2610)* lines. D) Western blot of total protein probed with a α -SUMO antibody. Bands represent the collection of proteins SUMOylated in adult worms.

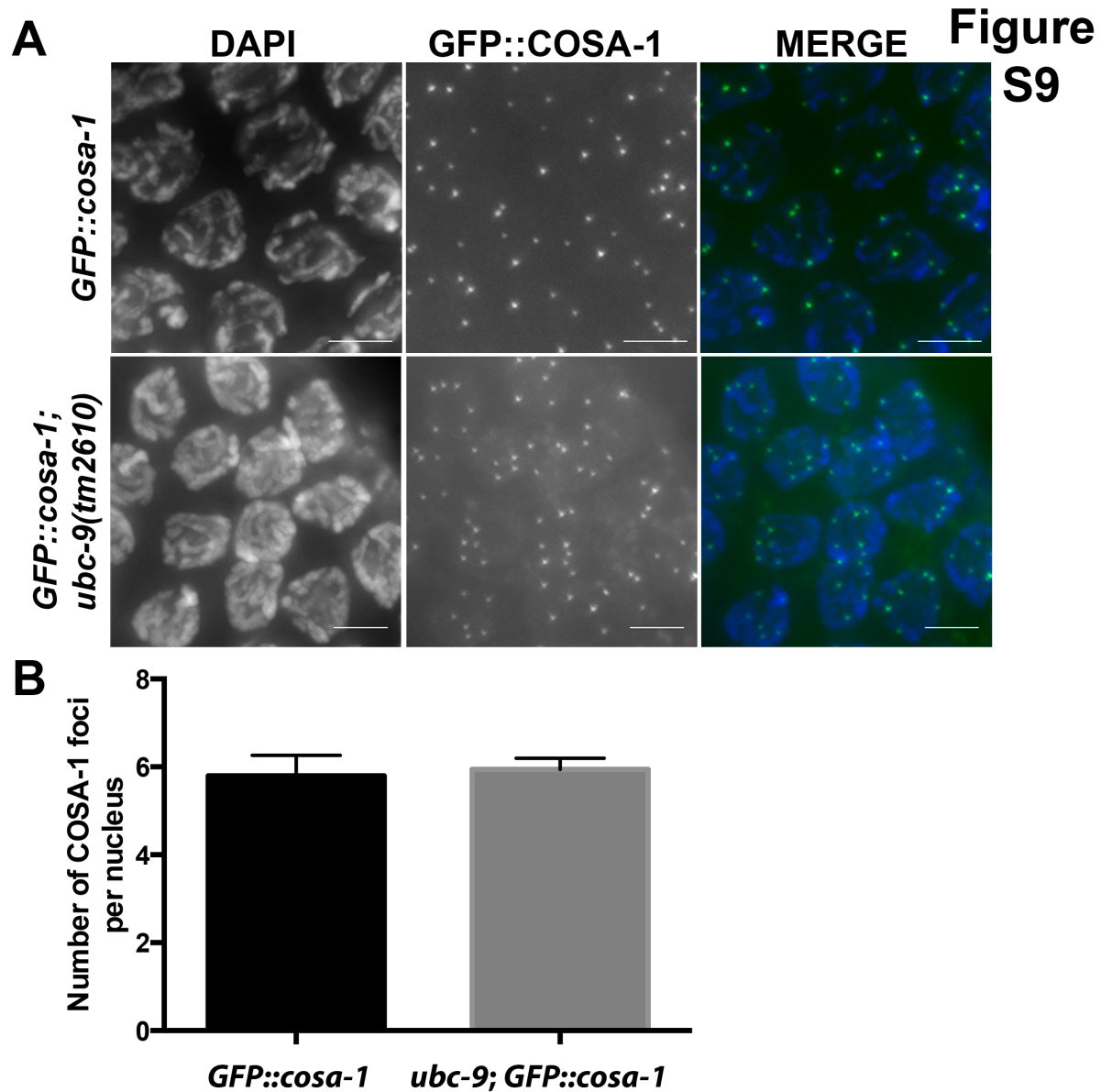


Supplemental Figure 7: MRE-11 localization is not affected in *ubc-9(tm2610)* mutants. GFP was visualized by fixing worms without antibody addition. MRE-11 localizes to the nucleus throughout prophase I. This localization does not change in *ubc-9(tm2610)* mutants. Polarized nuclei can still be seen in mid/late pachytene of *ubc-9* germlines, which is normal for this genotype.

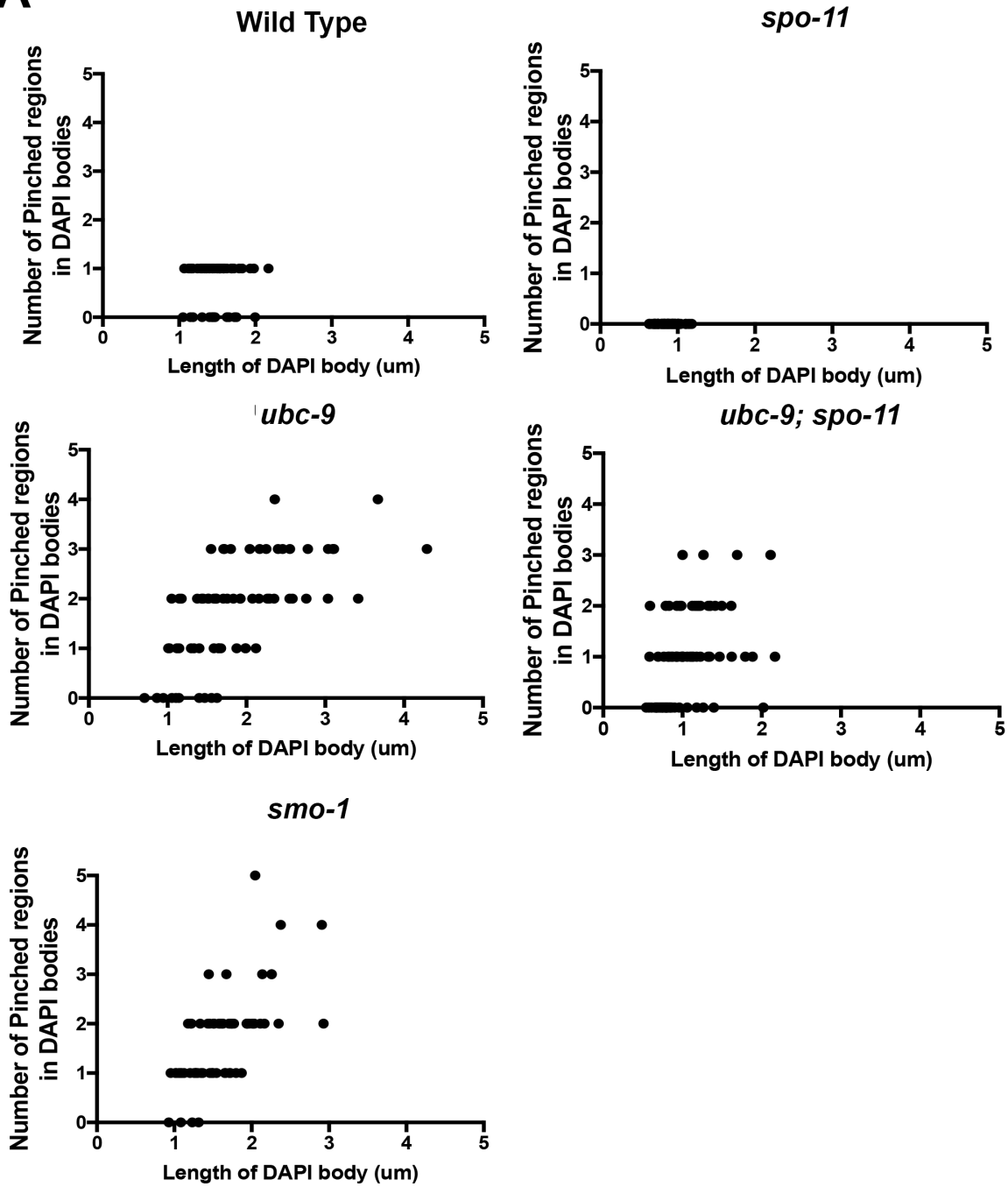
Figure S8



Supplemental Figure 8: UBC-9 localization is not altered when MRE-11 is absent from the germline. A 3XFLAG::UBC-9;*mre-11(ok179)* strain was analyzed for the location of UBC-9. This strain shows cytoplasmic staining, but nuclear localization of UBC-9 (see Figure 1) is no longer present. Error bars signify the mean \pm SEM.



Supplemental Figure 9: Interfering COs are unchanged in *ubc-9* mutants. A) *GFP::*COSA-1** in wild type and *ubc-9* mutant strains. Images were taken in late pachytene. Green: *GFP::*COSA-1**, Blue: DAPI. B) Numbers of *COSA-1* foci in late pachytene, just before diplotene. There is no significant difference between numbers of *COSA-1* foci in WT vs. *ubc-9* mutants ($p=0.84$). 78 WT nuclei were counted from three germlines, and 128 *ubc-9(tm2610)* nuclei were counted from four germlines. Error bars signify the mean \pm SEM.

A

Supplemental Figure 10: Diakinesis DAPI body length increases with the number of pinched regions observed. A) Scatterplot of each genotype comparing the length of DAPI body to the number of pinched regions within that DAPI body. Wild type has one pinched region per bivalent, but because of bivalent orientation, some pinched regions could not be viewed and thus

are counted as 0. *spo-11* mutants have univalents with no visible pinched regions, and thus are counted as 0. SUMOylation mutants have increased numbers of pinched regions in some DAPI bodies, and these have increased length. *ubc-9; spo-11* double mutants have an intermediate phenotype.